Kinetic Characterization of Human JNK2α2 Reaction Mechanism Using Substrate Competitive Inhibitors

Linghao Niu,[‡] Kung-Ching Chang,[§] Stacy Wilson,[§] Patricia Tran,[‡] Fengrong Zuo,[§] and David C. Swinney*[,‡]

Departments of Biochemical Pharmacology, and Inflammation, Autoimmunity and Transplantation, Roche Palo Alto LLC, 3431 Hillview Avenue, Palo Alto, California 94304

Received November 22, 2006; Revised Manuscript Received January 30, 2007

ABSTRACT: Jun N-terminal kinase (JNK) is a stress activated serine/threonine protein kinase that phosphorylates numerous cellular protein substrates including the transcription factors c-Jun and ATF2. In this study, we defined the kinetic mechanism for the active form of JNK2α2. Double reciprocal plots of initial rates versus concentrations of substrate revealed the sequential nature of the JNK2α2 catalyzed ATF2 phosphorylation. Dead-end JNK inhibitors were then used to differentiate ordered and random kinetic mechanisms for the reaction. A peptide inhibitor containing the homology JNK docking sequence for substrate recognition, derived from amino acid residues 153−163 of JNK-interacting protein 1 (JIP-1), inhibited JNK activity via competition with ATF2. This peptide functioned as a noncompetitive inhibitor against ATP. In contrast, the anthrapyrazolone compound, SP600125, exhibited competitive inhibition for ATP and noncompetitive inhibition against ATF2. Furthermore, binding of one substrate had no significant effect on the affinity for the other substrate. The data in this study are consistent with a kinetic mechanism for activated JNK2α2 in which (1) substrate binding is primarily due to the distal contacts in the JNK2α2 docking groove that allow the delivery of the substrate phosphorylation sequence into the catalytic center, (2) there is minimal allosteric communication between the protein−substrate docking site and the ATP binding site in the catalytic center for activated JNK2α2, and (3) the reaction proceeds via a random sequential mechanism.

The c-Jun N-terminal kinases (JNKs[1]) are stress-activated protein kinases that can be induced by inflammatory cytokines, environmental stress, UV radiation, and mitogens (*1*−*6*). As such, JNK inhibitors have the potential to be immuno-modulatory agents. A greater understanding of JNK enzymology may provide insights into efforts focused on developing JNK inhibitors as immuno-modulatory agents.

JNKs belong to the mitogen-activated protein kinase (MAPK) family, encoded by three distinct genes, JNK1, JNK2, and JNK3 (*7*). JNK1 and JNK2 genes are ubiquitously expressed, whereas JNK3 expression is primarily localized in neuronal tissues and cardiac myocytes (*8*). JNK is a serine/threonine protein kinase with 11 subdomains (*7*). Alternative splicing at two major sites yielded 10 JNK variants: (1) splicing at the C-terminus created isoforms that differ in length with unknown functional significance; (2) the alternative splicing within subdomains IX and X resulted in α- and β-isoforms with distinct substrate selectivity (*7*, *9*, *10*). High sequence homology was found within the region spanning the kinase domains among JNKs (*7*, *10*, *11*). Specifically, JNK3 shares 92% and 87% identical amino acids with JNK1 and JNK2, respectively (*11*).

JNK activation is cooperatively mediated by MKK4 and MKK7 through dual phosphorylation of the Thr-Pro-Tyr motif located in the activation loop (*12*−*14*). JNK also contains a conserved common docking domain in the near C-terminal region (as do other members of the MAPK family) that is distant from the catalytic site (*15*). This docking site mediates JNK binding with its interacting proteins including substrates, upstream kinases and phosphatases (*16*). Activated JNK interacts with a number of cellular protein substrates including transcription factors c-Jun and ATF2 (*17*). Phosphorylation of c-Jun results in dimerization to form activator protein-1 (AP-1). In complex with other DNA-binding proteins, AP-1 regulates the transcription of numerous inflammatory genes, including tumor necrosis factor alpha (TNF-α), interleukin 2 (IL-2) and matrix metalloproteinases (*18*−*21*). In addition to its role in inflammation, activation of the JNK pathway has also been implicated in cancer (*22*), neurodegeneration (*23*), and diabetes (*24*). Gene-disruption and functional-interference studies provided some clues to the diverse context-specific activities of JNKs (*25*). Multiple JNK isoforms have been found in association of various human diseases (*26*).

JNK docks with specific scaffold proteins, known as JNK-interacting proteins (JIPs), to form functional signaling modules in cells (*27*−*30*). JIPs provide a scaffold to facilitate the activation of JNK by upstream kinases. A small peptide

* To whom correspondence should be addressed. Phone: (650) 855-5349. Fax: (650) 852-3111. E-mail: david.swinney@roche.com.

‡ Department of Biochemical Pharmacology.

§ Department of Inflammation, Autoimmunity and Transplantation.

[1] Abbreviations: JNK, Jun N-terminal kinase; ATF2, activating transcription factor 2; ATP, adenosine triphosphate; JIP, JNK-interacting protein; MAPK, mitogen-activated protein kinase; MEK, MAPK/ERK kinase; MKK, MAP kinase kinase; MAPKKK, MAP kinase kinase kinase; AP-1, activator protein-1; BSA, bovine serum albumin; DTT, dithiothreitol; GST, glutathione *S*-transferase; EDTA, ethylenediaminetetraacetic acid; HEPES, *N*-(2-hydroxyethyl)piperazine-*N*′-2-ethanesulfonic acid.

10.1021/bi602423e CCC: $37.00
Published on Web 03/31/2007

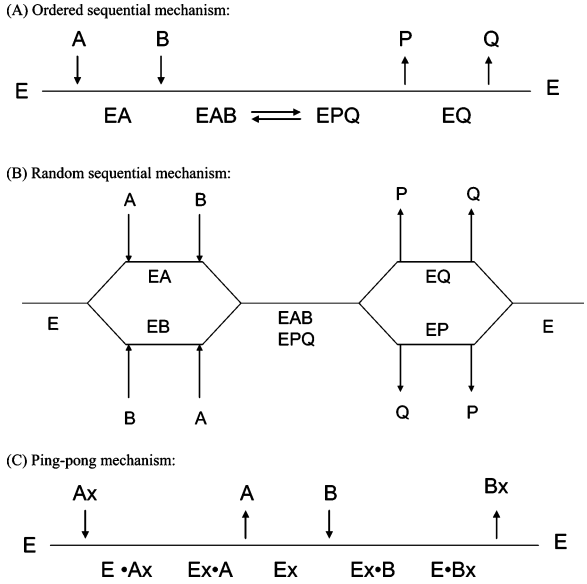

FIGURE 1: Kinetic mechanisms for enzyme-catalyzed two-substrate reactions. (A) Sequential, ordered mechanism. (B) Sequential, random mechanism. (C) Ping−pong mechanism.

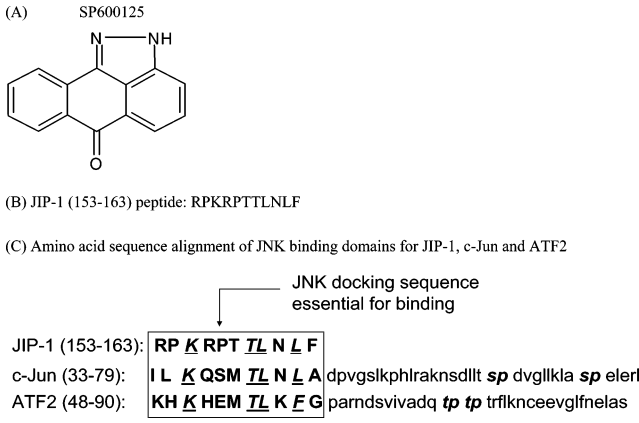

FIGURE 2: Dead-end substrate competitive inhibitors used in this study for JNK kinetic mechanism investigation. (A) Structure for SP600125. (B) Peptide inhibitor for JNK, JIP-1 (153−163). (C) Amino acid sequence alignment of JNK binding domains for JIP-1, c-Jun, and ATF2. The consensus amino acids in JNK docking domains are underlined in italic in the boxed region. The phosphorylation residues in c-Jun and ATF2 by JNK are shown in bold, italic font.

containing amino acids 153−163 of JNK-interacting protein-1 (JIP-1) has been found to inhibit JNK activity (*31*). Crystal structure analysis demonstrated that this peptide inhibitor binds in the conserved common docking groove of JNK that is important for substrate binding (*32*).

An in-depth understanding of the enzymatic mechanism of JNK-catalyzed phosphorylation is important to facilitate the discovery of specific JNK inhibitors. JNK catalyzes a two-substrate reaction that involves the transfer of the γ-phosphate group of ATP to the protein substrate followed by the release of ADP and the phosphorylated protein. Figure 1 shows the possible kinetic models for a bi-substrate system. In ordered sequential reactions (Figure 1A), the enzyme binds substrates and releases products in a specific order. In random mechanisms (Figure 1B), there is no obligatory order for the addition of substrates and the dissociation of products. Ordered and random sequential models require both substrates to be bound to the enzyme in a ternary complex prior to chemical catalysis. However, in a ping−pong mechanism (Figure 1C), only one substrate can associate with the enzyme at a time. Upon dissociation of the first product, the second substrate binds to the enzyme followed by the release of the second product.

In order to better understand the mechanism of the JNK enzyme reaction, we conducted steady-state kinetics studies using active human JNK2α2 and the JNK-specific dead-end inhibitors, SP600125 (Figure 2A) and JIP-1 (153−163) peptide (Figure 2B). Because of the sequence homology between the JNK isoforms, JNK2α2 was considered representative of the family. SP600125 is an anthrapyrazolone compound identified by Celgene (*33*). Differentiation between random and ordered mechanisms for a sequential reaction requires the use of either dead-end inhibitors or product-inhibition studies (*34*−*36*). In product-inhibition analysis, the reversible link between the product and substrate can complicate the kinetic patterns (*35*). However, the dead-end enzyme−inhibitor complexes have the advantage in the study of the catalytic reaction in a single direction to avoid the complications caused by the reversible reaction in product-inhibition kinetics (*35*, *36*). Therefore, in this work, we chose to employ dead-end substrate competitors to define the JNK kinetic mechanism. The anthrapyrazolone compound, SP600125 binds into the ATP pocket on JNK and shuts down the phosphorylation reaction by forming a dead-end complex with the kinase. As a protein substrate analogue, JIP-1(153−163) peptide binds to the same docking site on JNK as the protein substrate. The peptide, however, functions as a dead-end inhibitor in JNK catalysis because of the absence of the JNK phosporylation site in its sequence. Because these dead-end inhibitors have no reversible connections with the substrates in the JNK reaction, they become valuable tools in making definitive conclusions in the JNK kinetic mechanism characterization. Our results indicated that JNK2α2-catalyzed substrate phosphorylation follows a sequential, random kinetic mechanism. Kinetic parameters indicated that there is no significant cooperative interaction between the binding sites for ATP and the protein substrate.

MATERIALS AND METHODS

Materials. [γ-^{33}P] ATP and glutathione sepharose 4B resin were purchased from GE Healthcare (Buckinghamshire, England). MultiScreen 96-well plates were purchased from Millipore (Burlington, MA). Anthra[1,9-*cd*]pyrazol-6(2*H*)-one (SP600125) and BSA were purchased from Sigma-Aldrich (St. Louis, MO). Dithiothreitol (DTT) was from Promega (Madison, WI). ATP was from Roche Applied Science (Indianapolis, IN). Active mouse MKK4, active human MKK7α1, and inactive human JNK2α2 were purchased from Upstate (Lake Placid, NY). The JIP-1 (153−163) peptide, RPKRPTTLNLF, was synthesized by AnaSpec, Inc. (San Jose, CA).

Expression and Purification of Active Human JNK2α2. The recombinant, active human JNK2α2 kinase was generated in an *E. coli* expression system by coexpression of its two upstream kinases MAPKK (MEK4) and MAPKKK-(MEKK1) (*37*). cDNA expression plasmids encoding human MEK4 (pQE30-MEK4) and the constitutively active mutant protein of MEKK-1 (pBB131-MEKK1) were kindly provided

by Professor Cobb from the University of Texas at Southwestern Medical Center. The wild-type, full-length cDNA clone encoding human JNK2α2 was purchased from Origene Technologies, Inc. (Rockville, MD). By PCR amplification, the full-length cDNA encoding JNK2α2 and a bacterial ribosomal binding site (AGGAGA) were subcloned upstream of the full-length MEK4 cDNA fragment into the pQE30-MEK4 plasmid. The resulting pQE30-JNK2α2-MEK4 plasmid directed the expression of JNK2α2 with a His_6 tag and untagged MEK4.

The pQE30-JNK2α2-MEK4 plasmid was then transformed together with pBB131-MEKK1 into *Echerchia coli* Strain BL21 (Novagen, San Diego, CA). Expression of the active JNK2α2 in *E. coli* was induced with 0.25 mM IPTG for 4 h at 37 °C and then was purified by using Qiagen's His-tagged protein purification kit containing Ni-NTA superflow columns. Specifically, cell pellets were first sonicated in lysis buffer (50 mM NaH_2PO_4, 300 mM NaCl, 10 mM imidazole, 1× proteinase inhibitor cocktail without EDTA, 1 mM Na_3VO_4, and 0.5% NP-40 at pH 8.0) and then were clarified by centrifugation at 10,000*g* for 30 min. The supernatant was incubated with Ni^{2+}-NTA agarose beads (Qiagen, Valencia, CA) with gentle rocking at 4 °C for 1 h. The beads were then transferred to the Ni-NTA column (Qiagene, Valencia, CA) and washed with 20× column volume of washing buffer (50 mM NaH_2PO_4, 500 mM NaCl, 25 mM imidazole, 1× proteinase inhibitor cocktail without EDTA, 1 mM Na_3VO_4, and 0.5% NP-40 at pH 8.0). His-tagged JNK2α2 was finally eluted from the column with an elution buffer (50 mM NaH_2PO_4, 500 mM NaCl, 250 mM imidazole, 1× proteinase inhibitor cocktail without EDTA, 1 mM Na_3VO_4, and 0.05% NP-40 at pH 8.0) and dialyzed overnight against a storage buffer (50 mM Tris at pH 8.0, 150 mM NaCl, 1 mM DTT, 1 mM Na_3VO_4, 20% glycerol, and 0.05% NP-40). The aliquot of the purified, active JNK2α2 protein was stored in a −80 °C freezer.

ATF2 Expression and Purification. cDNA encoding truncated human ATF2 (amino acids 19−96) was generated from the human brain cDNA library (Clontech, Mountain View, CA) by PCR amplification, incorporating a 3′-stop codon. The amplified cDNA fragment was then sub-cloned into the bacterial expression plasmid pGEX-2T as a GST-fusion protein. The resulting plasmid, pGST-ATF2, was transformed into the competent *Echerchia coli* strain BL21 (Novagen, San Diego, CA). The expression of recombinant GST-ATF2 protein was induced by treating transformed cells for 5 h with 0.4 mM IPTG at 30 °C. The protein was then purified with glutathione-agarose columns (B-PER GST Spin Purification Kit, Pierce Rockford, IL) according to the manufacturer's protocol. The eluted protein was then dialyzed against a storage buffer containing 100 mM NaCl, 50 mM HEPES (pH 7.4), 5% glycerol, 1 mM DTT, and a protease inhibitor cocktail (Roche Applied Science, Indianapolis, IN).

Activation of Human JNK2α2 in Vitro by MKK4 and MKK7α1. All *in vitro* activation reactions for human JNK2α2 by upstream kinases, MKK4 and MKK7, were conducted at 30 °C for 30 min. In the MKK4-catalyzed JNK activation reaction, 1 μg of human JNK2α2 protein, inactive (Upstate, Lake Placid, NY) or active (this work), was incubated with 100 ng of active mouse MKK4 (Upstate, Lake Placid, NY) in a volume of 40 μL in a buffer containing 50 mM Tris-HCl, at pH 7.5, 6.25 mM β-glycerol phosphate, 1.25 mM EGTA, 15 mM DTT, 0.25 mM sodium orthovanadate, 19 mM $MgCl_2$, and 125 μM ATP. For JNK activation by MKK7α1, the reaction was carried out by incubating 2 μg of human JNK2α2 protein, inactive (Upstate, Lake Placid, NY) or active (this work), with 1.5 μg of active human MKK7α1 (Upstate, Lake Placid, NY) in 40 μL in a buffer containing 20 mM MOPS at pH 7.2, 25 mM β-glycerol phosphate, 5 mM EGTA, 1 mM DTT, 1 mM sodium orthovanadate, 19 mM $MgCl_2$, and 125 μM ATP.

The specific enzyme activities of the human JNK2α2 proteins, treated with or without mouse MKK4 or human MKK7α1, were measured by the phosphorylation of GST-ATF2 (19−96) with [γ-^{33}P] ATP. The reaction was conducted with 60 μM ATP (10μCi [γ-^{33}P] ATP) and 6 μM ATF2 at final volume of 40 μL in a buffer containing 25 mM Hepes at pH 7.5, 2 mM dithiothreitol, 150 mM NaCl, 20 mM $MgCl_2$, 0.001% Tween 20, and 0.1% BSA. After 30 min of incubation at 30 °C, the reaction was terminated by adding 25 μL of 0.75% phosphoric acid. The reaction product was then captured on a P81 phosphocellulose membrane square filter (Upstate, Lake Placid, NY). The filters were washed with 0.75% phosphoric four times to remove the free radionucleotide. The incorporation of ^{33}P into ATF2 was quantified on a liquid scintillation counter (Packard, Meriden, CT).

JNK Enzyme Kinetic Assays. JNK activity was measured by the phosphorylation of GST-ATF2 using [γ-^{33}P] ATP at 30 °C in filtration assay format. The enzyme reaction was conducted in a volume of 40 μL in a buffer containing 25 mM Hepes at pH 7.5, 2 mM dithiothreitol, 150 mM NaCl, 20 mM $MgCl_2$, 0.001% Tween 20, and 0.1% BSA. The substrate kinetic profiles for the bi-substrate reaction were determined from the initial rates measured with 1 nM human JNK2α2 by varying the concentrations of one substrate while holding the other substrate at several constant concentrations. These assays typically contained GST-ATF2 in the concentration range of 0.2−7 μM, nonradioactive ATP in the range of 1−150 μM with 2−20 μCi [γ-^{33}P] ATP per reaction.

To define the mechanism of JNK inhibition, the inhibition assays were carried out by keeping one substrate at constant level of K_m while changing the concentration of the other substrate in the absence or presence of several fixed inhibitor concentrations. Typically, the reaction mixtures contained either the SP600125 or JIP-1(153−163) peptide in the range of 1− 10 μM with 1 nM human JNK2α2. The concentrations of the varied substrates in the inhibition assays were similar to the ranges used in substrate kinetics studies.

All kinetic reactions were initiated by the addition of enzyme and allowed to proceed, typically, for 30 min to ensure linearity. The conversion of the limiting substrate to product was never more than 10%. At the end of incubation, the reaction was terminated by transferring 25 μL of the reaction mixture to 150 μL of 20% glutathione sepharose slurry containing 135 mM EDTA. The reaction product was captured on the affinity resin and washed on a filtration plate with phosphate buffered saline six times to remove the unreacted radionucleotide. Then the incorporation of ^{33}P into ATF2 was quantified on a microplate scintillation counter (Packard Topcount, Meriden, CT).

Kinetic Data Analysis. The initial rates data from JNK catalyzed two-substrate kinetic profiles were fitted to eq 1

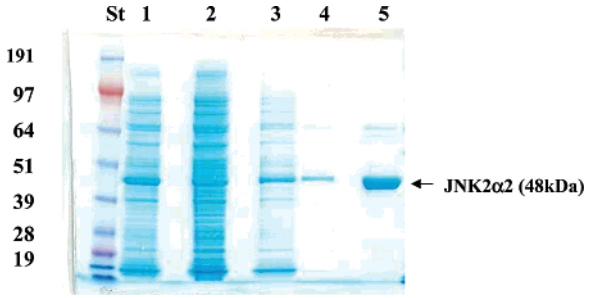

FIGURE 3: Human JNK2α2 affinity purification. *E. coli* BL21 cells expressing His-tagged active human JNK2α2 were disrupted by sonication. The cell lysate supernatant was loaded onto a Ni^{2+}-NTA agrose column for affinity purification as described in Materials and Methods. Lane 1, cell lysate supernatant; lane 2, flow-through from Ni^{2+}-NTA column loaded with cell lysate supernatant; lanes 3 and 4, initial and final wash, respectively, of the Ni^{2+}-NTA column loaded with cell lysate supernatant; lane 5, His-tagged JNK2α2 protein finally eluted from the Ni^{2+}-NTA column. The St lane contained molecular mass standards with indicated kDa values. Coomassie blue staining of a 4−12% NuPAGE gel (Invitrogen) is shown.

(sequential mechanism) and eq 2 (ping−pong mechanism) using GraphPad Prism, version 4.0.

$$v = V_{max}[A][B]/(K_{ma}[B] + K_{mb}[A] + [A][B] + K_{ia}K_{mb}) \quad (1)$$

$$v = V_{max}[A][B]/(K_{ma}[B] + K_{mb}[A] + [A][B]) \quad (2)$$

where A and B represent substrates, K_{ma} and K_{mb} are the Michaelis−Menton constants of the substrates, K_{ia} is the dissociation constant for substrate A from the free enzyme, and V_{max} is the maximum initial velocity.

The initial reaction rate data from JNK inhibition experiments were fitted to the competitive inhibition model (eq 3), the noncompetitive inhibition model (eq 4), and the uncompetitive inhibition model (eq 5).

$$v = V_{max}[S]/(K_m(1 + [I]/K_{is}) + [S]) \quad (3)$$

$$v = V_{max}[S]/(K_m(1 + [I]/K_{is}) + [S](1 + [I]/K_{ii})) \quad (4)$$

$$v = V_{max}[S]/(K_m + [S](1 + [I]/K_{ii})) \quad (5)$$

In these equations, V_{max} is the maximum velocity, K_m is the Michaelis−Menton constant for the varied substrate, S is the varied substrate, I is the inhibitor, and K_{is} and K_{ii} are the inhibition constants derived from the slope and y-intercept of Lineweaver−Burk plots, respectively. Data were analyzed on Microsoft Excel for parameter estimation.

RESULTS

Human JNK2α2 Affinity Purification and Activity Analysis. The recombinant human JNK2α2 kinase was expressed in active form in *E. coli* by coexpression with JNK upstream activation kinases as described in Materials and Methods. The His-tagged human JNK2α2 protein from the overexpression system was purified by affinity chromatography using an Ni-NTA superflow column according to the standard protocol (Qiagen). Figure 3 shows a highly purified band of human JNK2α2 protein around 48 kDa (lane 5) in the eluted fraction from the affinity column. The JNK preparation displayed greater than 90% purity on the basis of a Coomassie blue stained gel.

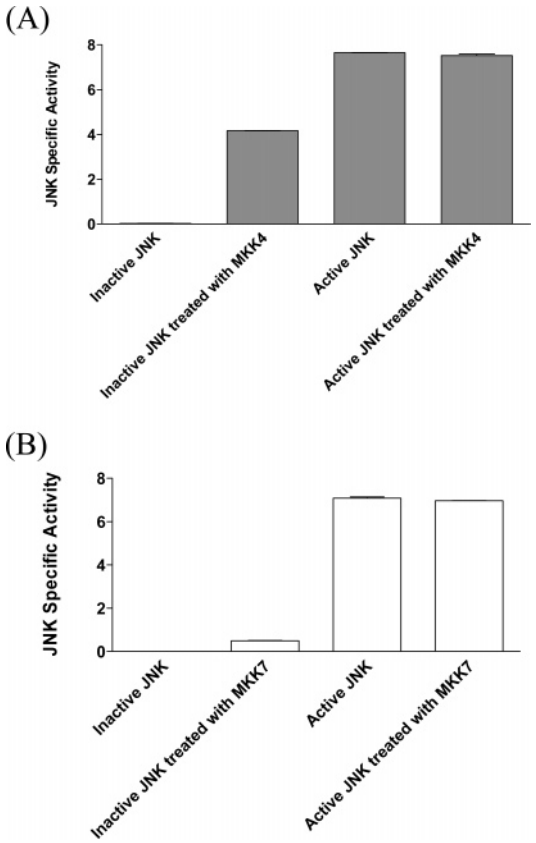

FIGURE 4: Human JNK2α2 *in vitro* activation by MKK4 and MKK7. (A) Purified active human JNK2α2 from this study or the inactive human JNK2α2 purchased from Upstate incubated with or without mouse MKK4. (B) Purified active human JNK2α2 from this study or the inactive human JNK2α2 from Upstate incubated with or without human MKK7α1. The specific activities of the JNK2α2 proteins were determined as pmol of phosphate transferred from ATP to ATF2 per pmol of JNK protein per min under the assay conditions described in Materials and Method. The error bars represent the standard error of the mean of duplicate determinations.

The purified human JNK2α2 preparation was further treated with JNK-specific upstream activation kinases, MKK4 and MKK7, to evaluate its activation status. These results were compared with the inactive human JNK2α2 enzyme purchased from Upstate. As shown in Figure 4A, the non-phosphorylated JNK2 from Upstate did not display any detectable enzyme activity. The MKK4 treatment activated the inactive JNK2 with a large increase of enzyme activity. However, the active JNK2α2 from our purified preparation displayed similar specific enzyme activity with or without MKK4 treatment. Similar conclusions were also obtained from the MKK7-catalyzed JNK2α2 activation experiment (Figure 4B). The lack of an additional increase in specific activity indicates that the human JNK2α2 protein from our expression system is fully activated.

Substrate Kinetic Profile of Bi-Reactant Phosphorylation Reaction Catalyzed by Human JNK. Kinetic mechanisms for enzymatic reactions with two substrates include two major categories: sequential and ping−pong. Distinctions between sequential versus ping−pong mechanisms can be made by analyzing initial rate data in Lineweaver−Burk plots when one substrate is varied at several fixed levels of the other substrate (*35*). Sequential mechanisms will exhibit a converging plot pattern, whereas ping−pong mechanisms will give rise to a family of parallel lines with a constant slope.

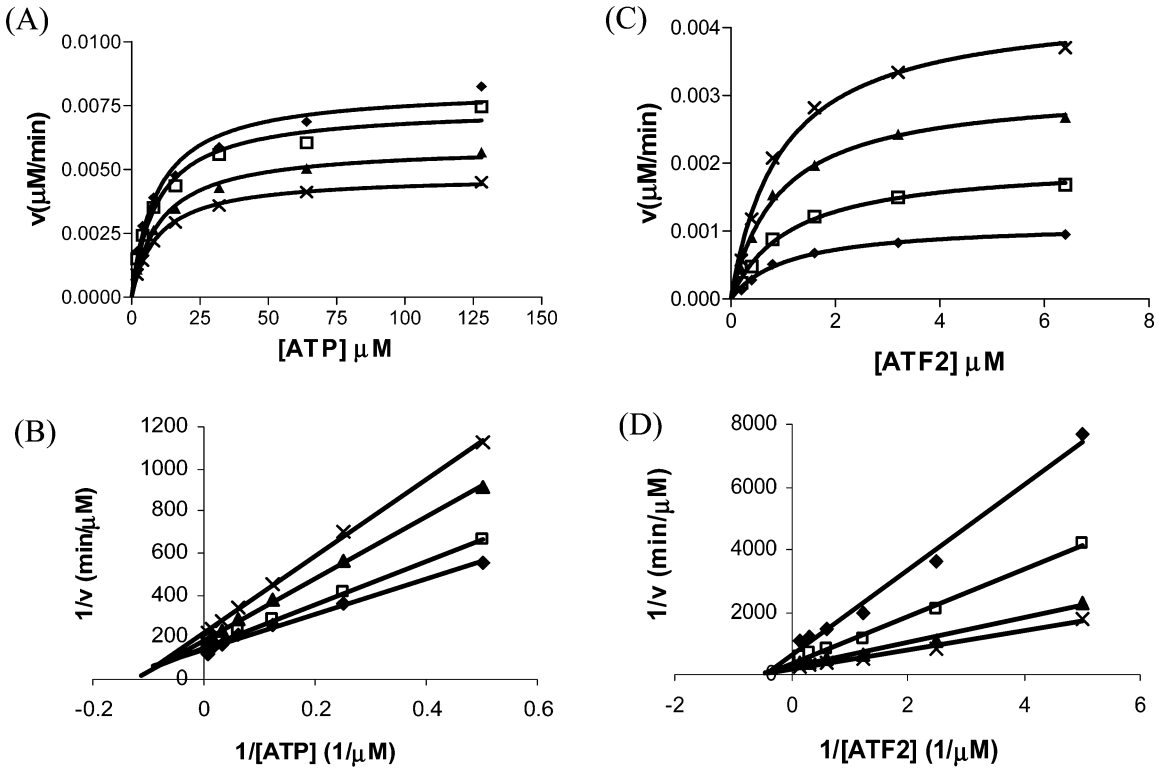

FIGURE 5: Substrate kinetic profiles of a JNK-catalyzed two-substrate reaction. (A) Plot of initial reaction rate as a function of ATP concentration at four fixed ATF2 concentrations of 0.6 μM (×), 0.8 μM (▲), 1.6μM (□), and 3.2 μM (♦). (B) Double-reciprocal plot of 1/rate vs 1/[ATP] at four fixed ATF2 concentrations of 0.6 μM (×), 0.8 μM (▲),1.6 μM (□), and 3.2 μM (♦). The best fit of the data with ATP as the varied substrate to eq 1 yielded a K_m of 0.54 μM and a K_{ia} of 1.2 μM for ATF2, and a K_m of 5.3 μM for ATP. (C) Plot of the initial reaction rate as a function of ATF2 concentration at four fixed ATP concentrations of 1 μM (♦), 2 μM (□), 4 μM (▲), and 8 μM (×). (D) Double-reciprocal plot of 1/rate vs 1/[ATF2] at four fixed ATP concentrations of 1 μM (♦), 2 μM (□), 4 μM (▲), and 8 μM (×). The best fit of the data with ATF2 as the varied substrate to eq 1 yielded a K_m of 4.1 μM and a K_{ia} of 10.2 μM for ATP, and a K_m of 1.1 μM for ATF2.

Table 1: Kinetic Constants for Human JNK2α2 from Two-Substrate Kinetics[a]

substrate	K_m (μM)	K_{ia} (μM)	k_{cat}[b] (min^{-1})
ATP	4.3 ± 0.9	10.1 ± 0.9	30.3 ± 3.6
GST-ATF2	0.8 ± 0.3	1.3 ± 0.2	

[a] The kinetic parameters were calculated from the data of three independent experiments using the equation for the sequential mechanism described under Kinetic Data Analysis. The standard deviations are shown. [b] The k_{cat} value, the catalytic constant of the enzyme, was calculated from V_{max} by using a known concentraion of JNK in the reaction ($V_{max} = k_{cat}$ [E]).

Steady-state kinetics studies were performed using ATP and the protein substrate ATF2 to differentiate between sequential and ping−pong mechanisms. Initial rates were determined at four fixed concentrations of ATF2 with varying ATP concentrations (Figure 5A and B). A family of similar plots was also generated from initial rates determined with varying concentrations of ATF2 at four fixed ATP concentrations (Figure 5C and D). The double-reciprocal plots of $1/v$ versus 1/[ATP] and $1/v$ versus 1/[ATF2] displayed converging line patterns. The results from three repeat experiments gave identical intersecting patterns in the reciprocal plots. The data best fit a sequential mechanism for the JNK reaction (eq 1). The average kinetic constants generated from these data are summarized in Table 1. The equilibrium dissociation constants for ATP and ATF2 from the free JNK enzyme (K_{ia}) are within 2-fold of their respective K_m values. The small difference in these parameters, most likely in the range due to experimental variation, suggests that there is no cooperativity between the ATP and protein substrate binding sites for activated JNK2α2. The insignificant substrate cooperativity was also reflected in the double reciprocal plots (Figure 5B and D), in which the family of lines intersect close to the *x*-axis, suggesting that affinities of ATP and ATF2 to the free enzyme are essentially the same as their K_m values. The sequential feature of the reaction suggests that JNK must bind both substrates, forming a ternary complex to proceed with catalysis.

Inhibition of JNK by SP600125. We then determined the substrate-binding order for the JNK reaction using dead-end substrate inhibitors. The inhibition effect of SP600125 on JNK was determined using both ATP and ATF2 as substrates. As shown in Figure 6, when using ATP as the variable substrate, the Lineweaver−Burk plots generated at several fixed inhibitor concentrations displayed a common intercept on the *y*-axis with slopes increasing linearly with inhibitor concentrations. This result indicated ATP's competitive inhibition of SP600125 for JNK2α2 with a K_{is} of 0.34 μM.

When the ATF2 concentration was varied in the presence of various constant levels of SP600125, the double-reciprocal plots revealed a noncompetitive inhibition pattern with a group of converging lines that intersected at a common point on the *x*-axis (Figure 7A). The plot of either the slope or *y*-intercept versus inhibitor concentration yielded a linear relationship with a K_{is} of 0.48 μM (Figure 7B) and a K_{ii} of 0.42 μM (Figure 7C). The inhibition pattern and the average inhibition constants of SP600125 are shown in Table 2. The

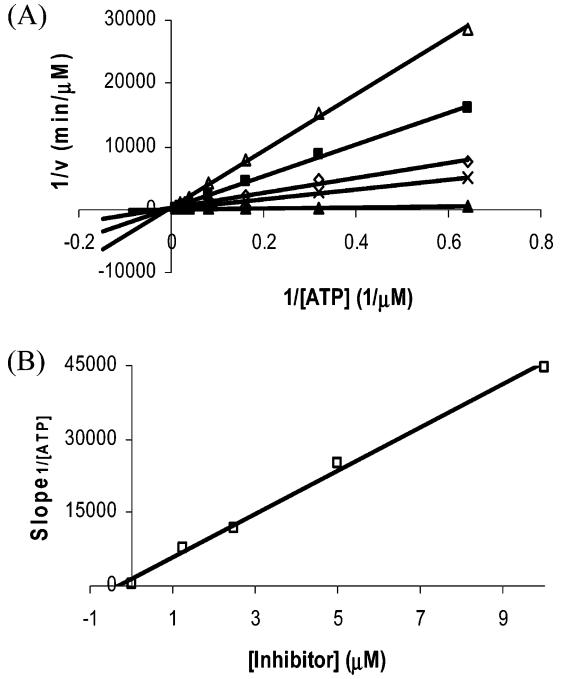

FIGURE 6: JNK inhibition pattern by SP600125 with ATP as the varied substrate. (A) Double-reciprocal plot of 1/rate vs 1/[ATP] at five fixed inhibitor concentrations of 0 μM (▲), 1.25 μM (×), 2.5 μM (◊), 5 μM (■), and 10 μM (△). (B) Re-plot of the slope from panel A vs inhibitor concentrations. The best fit of the data to competitive inhibition (eq 3) yielded a K_{is} of 0.34 μM.

noncompetitive inhibition pattern of SP600125 versus ATF2 clearly rules out the possibility that ATF2 binds as the first substrate in an ordered mechanism.

Inhibition of JNK by the JIP-1 (153−163) Peptide. A distinction of an ordered versus a random mechanism was made using a peptide inhibitor, JIP-1(153−163). Figure 8 shows the inhibition mode of JIP-1 (153−163) on JNK2α2. The common intersection point on the *y*-axis in the double-reciprocal plots of rate versus ATF2 concentration indicated that the inhibition was competitive against the protein substrate, with a K_{is} of 0.99 μM. The competitive result of the JIP-1 peptide with ATF2 revealed that the binding of the molecules is mutually exclusive and is consistent with them competing for a common docking groove on JNK2α2. These results support the idea that when JNK binds with its substrates, the protein−protein recognitions take place in the common docking site on JNK, where the JIP-scaffold proteins also interact.

Figure 9A demonstrates that the JIP-1 peptide (153−163) inhibited JNK noncompetitively versus ATP. Both the slope and *y*-intercept in the double-reciprocal plot changed linearly as a function of increasing concentration of the peptide inhibitor, resulting in a K_{is} of 0.88 μM (Figure 9B) and a K_{ii} of 0.97 μM (Figure 9C). The kinetic features of the JIP-1 peptide are summarized in Table 2. The noncompetitive mode of JIP peptide versus ATP further eliminated the possibility of an ordered mechanism with ATP as the first binding substrate for the JNK reaction. In that case, JIP-1 (153−163) would display uncompetitive inhibition against ATP, and the double-reciprocal plots would show a group of parallel lines with a constant slope at various fixed levels of the peptide inhibitor. Taken together, our data in this study suggest a sequential, random mechanism for the JNK-catalyzed phosphorylation reaction with no substantial cooperative interactions between the binding sites of ATP and the protein substrate.

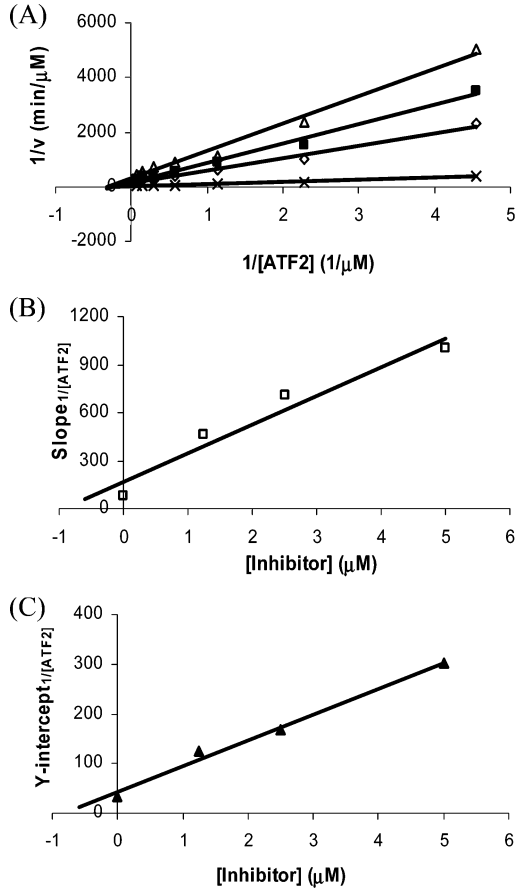

FIGURE 7: JNK inhibition pattern by SP600125 with ATF2 as the varied substrate. (A) Double-reciprocal plot of 1/rate vs 1/[ATF2] at four fixed inhibitor concentrations of 0 μM (×), 1.25 μM (◊), 2.5 μM (■), and 5 μM (△). (B) Re-plot of the slope from panel A vs inhibitor concentrations. The best fit of the data to noncompetitive inhibition (eq 4) yielded a K_{is} of 0.48 μM. (C) Re-plot of the *y*-intercept from panel A vs inhibitor concentrations. The best fit of the data to noncompetitive inhibition (eq 4) yielded a K_{ii} of 0.42 μM.

Table 2: Dead-End Inhibition Patterns and Inhibition Constants for Human JNK2α2[a]

inhibitor	variable substrate	inhibition mode	K_{is} (μM)	K_{ii} (μM)
SP600125	ATP	competitive	0.4 ± 0.1	N/A
SP600125	GST-ATF2	noncompetitive	0.5 ± 0.2	0.5 ± 0.1
JIP-1 (153−163)	GST-ATF2	competitive	1.1 ± 0.3	N/A
JIP-1 (153−163)	ATP	noncompetitive	1.6 ± 0.8	1.3 ± 0.3

[a] Each inhibition constant was calculated from data obtained in two identical experiments using the equation for either competitive or noncompetitive inhibition described under Kinetic Data Analysis. The average results are shown.

DISCUSSION

In this work, we used steady-state kinetics analysis to characterize the kinetic mechanism of active human JNK2α2. The intersecting plot pattern in substrate kinetic profiles revealed the sequential nature of the JNK2α2 reaction, indicating the involvement of a ternary complex in JNK catalysis. The substrate-binding order to JNK2α2 was determined using dead-end substrate competitive inhibitors.

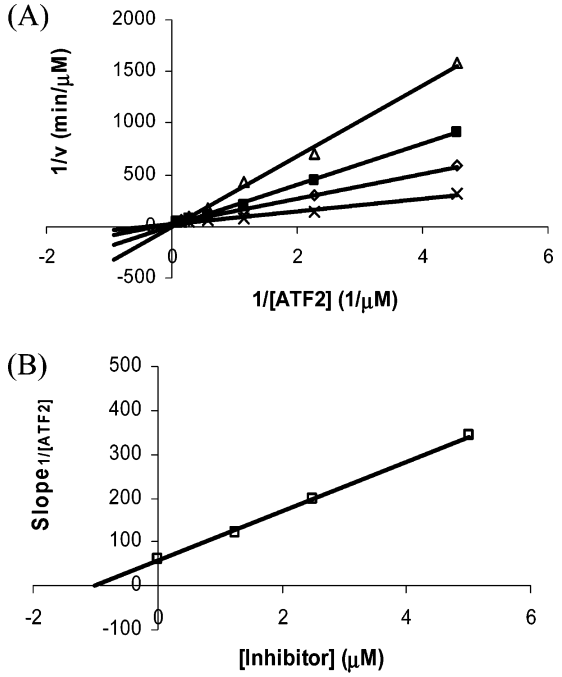

FIGURE 8: Inhibition of JNK by JIP-1(153−163) with ATF2 as the varied substrate. (A) Double-reciprocal plot of 1/rate vs 1/[ATF2] at four fixed inhibitor concentrations of 0 μM (×), 1.25 μM (◊), 2.5 μM (■), and 5 μM (△). (B) Re-plot of the slope from panel A vs inhibitor concentrations. The best fit of the data to competitive inhibition (eq 3) yielded a K_{is} of 0.99 μM.

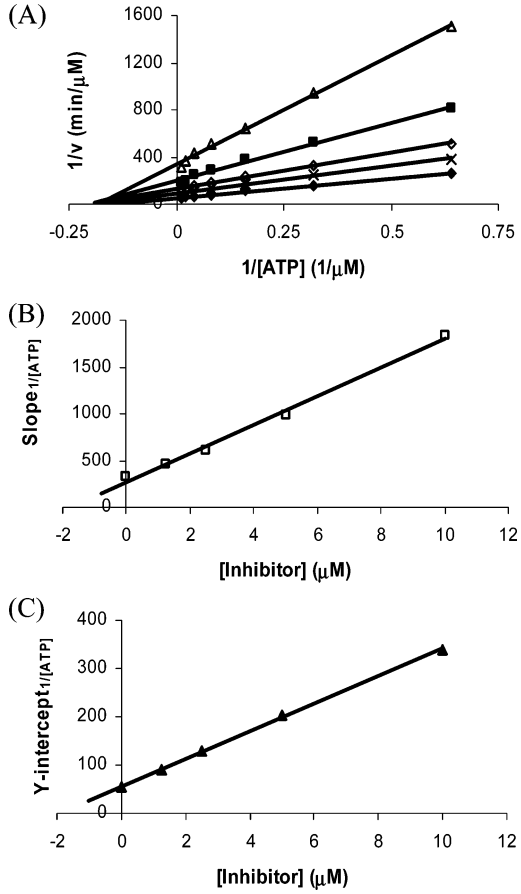

FIGURE 9: Inhibition of JNK by JIP-1 (153−163) with ATP as the varied substrate. (A) Double-reciprocal plot of 1/rate vs 1/[ATP] at five fixed inhibitor concentrations of 0 μM (♦), 1.25 μM (×), 2.5 μM (◊), 5 μM (■), and 10 μM (△). (B) Re-plot of the slope from panel A vs inhibitor concentrations. The best fit of the data to noncompetitive inhibition (eq 4) yielded a K_{is} of 0.88 μM. (C) Re-plot of the *y*-intercept from panel A vs inhibitor concentrations. The best fit of the data to noncompetitive inhibition (eq 4) yielded a K_{ii} of 0.97 μM.

Because of the absence of an uncompetitive inhibition pattern for either substrates, JNK2α2 must randomly bind ATP and ATF2 to form a ternary complex. Thus, the JNK-catalyzed phosphorylation reaction exhibits a sequential, random kinetic mechanism.

The inhibition data with JIP-1 (153−163) displayed a single competitive inhibition component against the substrate, ATF2. The pure competitive nature of ATF2 against JIP-1(153−163) is consistent with the hypothesis that the JIP-1 homology sequence plays an important role in the initial substrate docking interaction. What is the quantitative importance of this role? In our hands, the affinity of the JIP-1(153−163) peptide for the inhibition of JNK2α2 activity is 1.1 μM (Table 2), which is also similar to the dissociation constant for ATF2 binding to JNK2α2, 1.3 μM (Table 1). Bar and co-workers found that ATF2 and cJun peptides analogous to JIP-1(153−163) were less effective inhibitors of JNK activity than the JIP peptides (*31*). They observed 39 and 36% inhibition of JNK activity, respectively, using 1.7 μM peptide, suggesting that the K_i for the inhibition of JNK activity is in the low micromolar range. These data suggest that the JIP-1(153−163) peptide, ATF2 peptide, and ATF2 protein all bind to JNK with similar affinity. We also found the JIP-1 peptide to be competitive with c-Jun for JNK2α2 (data not shown). This has also been reported for the inhibition of JNK1α1 (*38*). These observations indicate that substrate binding utilizes the distal contacts in the JNK docking groove to mediate substrate recognition and that the substrate structure in the near vicinity of the phosphorylation site contributes little to substrate binding energy. Consistent with this binding model, a high affinity peptide substrate based on the phosphorylation elements in ATF2 or c-Jun has yet to be reported. By itself, the sequence flanking the phosphorylation site on a substrate usually exhibits poor kinase binding capability (*39*−*41*). The competitive inhibition of JIP-1 (153−163) against ATF2 eliminated the possibility that the local phosphorylation sequence on the JNK substrate independently binds into JNK phosphorylation catalytic site without the docking element. If that were to occur, the JIP-1 peptide would exhibit mixed type (noncompetitive) inhibition with respect to ATF2 because of the separated binding location of the JIP-1 peptide and substrate on JNK. These data are consistent with a model of substrate binding to JNK in which the majority of the initial binding energy results from interactions distal to the catalytic site with minimal contribution from the proximal substrate phosphorylation sequence. This mechanism is similar to substrate docking events described for other MAP kinases (*42*).

Information on the cooperative interaction between the binding sites for ATP and the protein substrate can be ascertained from the ratio of K_m/K_{ia}. In a sequential bi-substrate reaction, the K_m of a substrate is determined from the initial rate data when the enzyme is saturated with the other substrate. K_{ia} is defined as the equilibrium dissociation constant of the substrate from the free enzyme. The dissociation constants for inhibitor release from the free enzyme or the binary enzyme−substrate complex, K_{is} and K_{ii},

respectively, define the ability of the substrate to alter the binding site for the inhibitor (*34*, *43*). In this study, an approximately 2-fold difference was observed between K_{ia} and K_m for both ATP and ATF2. This difference may reflect a slightly increased binding affinity for one substrate in the presence of the other substrate (Table 1). However, in the JNK inhibition analysis using SP600125 and JIP-1 peptide, the values of K_{is} and K_{ii} were essentially the same (Table 2), indicating that there is no substantial cooperative interaction between the ATP site and the substrate docking site on JNK2α2. Similar results were observed with JNK1α1, which showed that the JIP-1 peptide had a similar affinity for JNK and that JNK complexed with ATP (*38*). These results are in contrast to the results of Heo et al. (*32*) that showed that the binding of the same JIP-1 peptide decreased the affinity of JNK1 for ATP. Using ITC, they observed an approximately 3-fold decrease in affinity for ATP upon the binding of the JIP-1 peptide. Structural studies supported these findings, that is, peptide binding was observed to induce a hinge motion between N-terminal and C-terminal domains of JNK and distortion of the ATP binding cleft. They also found a similar affinity of the JIP-1 peptide for JNK1, 0.42 μM, using ITC to measure direct binding, as reported here for the JIP-1 inhibition of the steady-state phosphorylation of ATF2 by JNK2α2 (1.1 μM). Barr and co-workers (*31*) also observed the K_d value for the JNK2-JIP peptide interaction to be in the low micromolar range using surface plasmon resonance/BIAcore technology.

A major distinction between this study and the one by Heo et al. is that this study used activated JNK2α2, whereas the study by Heo used inactivated JNK1α1. It is possible that the different results are due to a difference in the human JNK isoforms generated from the alternative splicing of three JNK genes; however, they share highly conserved sequence homology with similar overall structure (*11*, *32*). An alternative explanation for the differences between the two studies relates to the structure of the ATP binding site in activated versus inactivated JNKs. Comparing the results suggests that ATP binds a little more tightly to the activated form (4.3 μM) than the inactivated form (19 μM). Binding in the substrate docking domain decreases the affinity of ATP for the inactivated enzyme but has no effect on the affinity of ATP for the activated enzyme. Heo and co-workers proposed a model for JNK, where JIP binds to induce a conformational change in the catalytic binding site that increases the conformational flexibility of the loop containing the phosphorylation motif. The release of the phosphorylation loop, when JNK binds to the JIP1-scaffolding protein, may give a chance for the loop to refold and take an appropriate conformation to be recognized and phosphorylated by MKKs. If this is an accurate model for activation, then it is not surprising that the activated form of JNK does not require allosteric regulation through the binding of JIP1. Therefore, we propose that the allosteric inhibition mechanism proposed by Heo and co-workers is the specific property of the activation process of JNKs and is not observed for the fully activated JNK enzymes.

We observed a random, sequential mechanism for JNK-catalyzed phosphorylation using a truncated version of the protein substrate, ATF2 (19−96). Both random, sequential mechanisms (*44*−*51*) and the ordered mechanism have been reported for protein kinases (*52*, *53*). It has been noted that the order of substrate binding to a kinase can be affected by the substrate used in the investigation (*50*, *54*−*56*). p38, a well studied MAP kinase, displayed an ordered, sequential mechanism with the protein substrate ATF2 binding first (*53*). However, when using a peptide substrate, ATP was observed to bind first (*52*). The authors proposed that p38 presents a random binding opportunity for the substrates and that the preferred order is highly dependent on the phosphoryl acceptor. Clearly, JNK differs from p38 in having a random mechanism when the protein substrate ATF2 is used. Interestingly, the Michaelis constant for ATF2 binding to p38 was 12-fold greater than the dissociation constant, indicating that the binding of ATP affected the binding of GST-ATF2. The random mechanism for the JNK2α2 binding of ATP and ATF2 is consistent with the lack of cooperativity between the docking domain for the protein substrate and the ATP site in the catalytic center of JNK2α2.

A basic understanding of kinetic characteristics of an enzyme target is required to establish sensitive methods to detect inhibition. In this work, we revealed that the JNK2α2 reaction proceeds with a random, sequential mechanism. JNK can associate with analogue inhibitors in the presence and absence of the protein substrate or ATP. Therefore, both catalytic and direct binding assays will be appropriate for JNK inhibitor development.

The data in this study are consistent with a kinetic mechanism for activated JNK in which (1) substrate binding is primarily due to the distal contacts in the JNK2α2 docking groove that allow the delivery of the substrate phosphorylation sequence into the catalytic center, (2) there is minimal allosteric communication between the protein substrate docking site and the ATP binding site in the catalytic center for activated JNK2α2, in contrast to what is observed with the inactivated JNK1, and (3) the reaction proceeds via a random sequential mechanism.

ACKNOWLEDGMENT

We thank J. Michael Bradshaw, Eva Papp, Mohammad Hekmat-Nejad, and Holly Fleshman for the critical reading of the manuscript.

REFERENCES

1. Derijard, B., Hibi, M., Wu, I. H., Barrett, T., Su, B., Deng, T., Karin, M., and Davis, R. J. (1994) JNK1: a protein kinase stimulated by UV light and Ha-Ras that binds and phosphorylates the c-Jun activation domain, *Cell 76*, 1025−1037.
2. Kyriakis, J. M., Banerjee, P., Nikolakaki, E., Dai, T., Rubie, E. A., Ahmad, M. F., Avruch, J., and Woodgett, J. R. (1994) The stress-activated protein kinase subfamily of c-Jun kinases, *Nature 369*, 156−160.
3. Minden, A., Lin, A., Smeal, T., Derijard, B., Cobb, M., Davis, R., and Karin, M. (1994) c-Jun N-terminal phosphorylation correlates with activation of the JNK subgroup but not the ERK subgroup of mitogen-activated protein kinases, *Mol. Cell. Biol. 14*, 6683−6688.
4. Adler, V., Schaffer, A., Kim, J., Dolan, L., and Ronai, Z. (1995) UV irradiation and heat shock mediate JNK activation via alternate pathways, *J. Biol. Chem. 270*, 26071−26077.
5. Cano, E., Hazzalin, C. A., and Mahadevan, L. C. (1994) Anisomycin-activated protein kinases p45 and p55 but not mitogen-activated protein kinases ERK-1 and -2 are implicated in the induction of c-fos and c-jun, *Mol. Cell. Biol. 14*, 7352−7362.
6. Westwick, J. K., Weitzel, C., Minden, A., Karin, M., and Brenner, D. A. (1994) Tumor necrosis factor alpha stimulates AP-1 activity through prolonged activation of the c-Jun kinase, *J. Biol. Chem. 269*, 26396−26401.

7. Gupta, S., Barrett, T., Whitmarsh, A. J., Cavanagh, J., Sluss, H. K., Derijard, B., and Davis, R. J. (1996) Selective interaction of JNK protein kinase isoforms with transcription factors, *EMBO J. 15*, 2760−2770.
8. Martin, J. H., Mohit, A. A., and Miller, C. A. (1996) Developmental expression in the mouse nervous system of the p493F12 SAP kinase, *Brain Res. Mol. Brain Res. 35*, 47−57.
9. Chen, N., She, Q. B., Bode, A. M., and Dong, Z. (2002) Differential gene expression profiles of Jnk1- and Jnk2-deficient murine fibroblast cells, *Cancer Res. 62*, 1300−1304.
10. Kallunki, T., Su, B., Tsigelny, I., Sluss, H. K., Derijard, B., Moore, G., Davis, R., and Karin, M. (1994) JNK2 contains a specificity-determining region responsible for efficient c-Jun binding and phosphorylation, *Genes Dev. 8*, 2996−3007.
11. Xie, X., Gu, Y., Fox, T., Coll, J. T., Fleming, M. A., Markland, W., Caron, P. R., Wilson, K. P., and Su, M. S. (1998) Crystal structure of JNK3: a kinase implicated in neuronal apoptosis, *Structure 6*, 983−991.
12. Davis, R. J. (1999) Signal transduction by the c-Jun N-terminal kinase, *Biochem. Soc. Symp. 64*, 1−12.
13. Cuenda, A. (2000) Mitogen-activated protein kinase kinase 4 (MKK4), *Int. J. Biochem. Cell Biol. 32*, 581−587.
14. Hirai, S., Noda, K., Moriguchi, T., Nishida, E., Yamashita, A., Deyama, T., Fukuyama, K., and Ohno, S. (1998) Differential activation of two JNK activators, MKK7 and SEK1, by MKN28-derived nonreceptor serine/threonine kinase/mixed lineage kinase 2, *J. Biol. Chem. 273*, 7406−7412.
15. Tanoue, T., Adachi, M., Moriguchi, T., and Nishida, E. (2000) A conserved docking motif in MAP kinases common to substrates, activators and regulators, *Nat. Cell Biol. 2*, 110−116.
16. Enslen, H., and Davis, R. J. (2001) Regulation of MAP kinases by docking domains, *Biol. Cell. 93*, 5−14.
17. Minden, A., and Karin, M. (1997) Regulation and function of the JNK subgroup of MAP kinases, *Biochim. Biophys. Acta 1333*, F85−F104.
18. Jain, J., Valge-Archer, V. E., and Rao, A. (1992) Analysis of the AP-1 sites in the IL-2 promoter, *J. Immunol. 148*, 1240−1250.
19. Foletta, V. C., Segal, D. H., and Cohen, D. R. (1998) Transcriptional regulation in the immune system: all roads lead to AP-1, *J. Leukocyte Biol. 63*, 139−152.
20. Pendas, A. M., Balbin, M., Llano, E., Jimenez, M. G., and Lopez-Otin, C. (1997) Structural analysis and promoter characterization of the human collagenase-3 gene (MMP13), *Genomics 40*, 222−233.
21. Manning, A. M., and Mercurio, F. (1997) Transcription inhibitors in inflammation, *Expert Opin. Invest. Drugs 6*, 555−567.
22. Adjei, A. A. (2001) Blocking oncogenic Ras signaling for cancer therapy, *J. Natl. Cancer Inst. 93*, 1062−1074.
23. Bruckner, S. R., Tammariello, S. P., Kuan, C. Y., Flavell, R. A., Rakic, P., and Estus, S. (2001) JNK3 contributes to c-Jun activation and apoptosis but not oxidative stress in nerve growth factor-deprived sympathetic neurons, *J. Neurochem. 78*, 298−303.
24. Hirosumi, J., Tuncman, G., Chang, L., Gorgun, C. Z., Uysal, K. T., Maeda, K., Karin, M., and Hotamisligil, G. S. (2002) A central role for JNK in obesity and insulin resistance, *Nature 420*, 333−336.
25. Waetzig, V., and Herdegen, T. (2005) Context-specific inhibition of JNKs: overcoming the dilemma of protection and damage, *Trends Pharmacol. Sci. 26*, 455−461.
26. Manning, A. M., and Davis, R. J. (2003) Targeting JNK for therapeutic benefit: from junk to gold? *Nat. Rev. Drug Discovery 2*, 554−565.
27. Ito, M., Yoshioka, K., Akechi, M., Yamashita, S., Takamatsu, N., Sugiyama, K., Hibi, M., Nakabeppu, Y., Shiba, T., and Yamamoto, K. I. (1999) JSAP1, a novel jun N-terminal protein kinase (JNK)-binding protein that functions as a Scaffold factor in the JNK signaling pathway, *Mol. Cell. Biol. 19*, 7539−7548.
28. Whitmarsh, A. J., Cavanagh, J., Tournier, C., Yasuda, J., and Davis, R. J. (1998) A mammalian scaffold complex that selectively mediates MAP kinase activation, *Science 281*, 1671−1674.
29. Yasuda, J., Whitmarsh, A. J., Cavanagh, J., Sharma, M., and Davis, R. J. (1999) The JIP group of mitogen-activated protein kinase scaffold proteins, *Mol. Cell. Biol. 19*, 7245−7254.
30. Morrison, D. K., and Davis, R. J. (2003) Regulation of MAP kinase signaling modules by scaffold proteins in mammals, *Annu. Rev. Cell Dev. Biol. 19*, 91−118.
31. Barr, R. K., Kendrick, T. S., and Bogoyevitch, M. A. (2002) Identification of the critical features of a small peptide inhibitor of JNK activity, *J. Biol. Chem. 277*, 10987−10997.
32. Heo, Y. S., Kim, S. K., Seo, C. I., Kim, Y. K., Sung, B. J., Lee, H. S., Lee, J. I., Park, S. Y., Kim, J. H., Hwang, K. Y., Hyun, Y. L., Jeon, Y. H., Ro, S., Cho, J. M., Lee, T. G., and Yang, C. H. (2004) Structural basis for the selective inhibition of JNK1 by the scaffolding protein JIP1 and SP600125, *EMBO J. 23*, 2185−2195.
33. Bennett, B. L., Sasaki, D. T., Murray, B. W., O'Leary, E. C., Sakata, S. T., Xu, W., Leisten, J. C., Motiwala, A., Pierce, S., Satoh, Y., Bhagwat, S. S., Manning, A. M., and Anderson, D. W. (2001) SP600125, an anthrapyrazolone inhibitor of Jun N-terminal kinase, *Proc. Natl. Acad. Sci. U.S.A. 98*, 13681−13686.
34. Copeland, R. A. (2000) *Enzymes: A Practical Introduction to Structure, Mechanism, and Data Analysis*, 2nd ed., Wiley & Sons, New York.
35. Palmer, T. (1995) *Understanding Enzymes*, 4th ed., Prentice Hall, London.
36. Fromm, H. J. (1979) Use of competitive inhibitors to study substrate binding order, *Methods Enzymol. 63*, 467−486.
37. Khokhlatchev, A., Xu, S., English, J., Wu, P., Schaefer, E., and Cobb, M. H. (1997) Reconstitution of mitogen-activated protein kinase phosphorylation cascades in bacteria. Efficient synthesis of active protein kinases, *J. Biol. Chem. 272*, 11057−11062.
38. Barr, R. K., Boehm, I., Attwood, P. V., Watt, P. M., and Bogoyevitch, M. A. (2004) The critical features and the mechanism of inhibition of a kinase interaction motif-based peptide inhibitor of JNK, *J. Biol. Chem. 279*, 36327−36338.
39. Hawkins, J., Zheng, S., Frantz, B., and LoGrasso, P. (2000) p38 map kinase substrate specificity differs greatly for protein and peptide substrates, *Arch. Biochem. Biophys. 382*, 310−313.
40. Schulman, B. A., Lindstrom, D. L., and Harlow, E. (1998) Substrate recruitment to cyclin-dependent kinase 2 by a multipurpose docking site on cyclin A, *Proc. Natl. Acad. Sci. U.S.A. 95*, 10453−10458.
41. Brown, N. R., Noble, M. E., Endicott, J. A., and Johnson, L. N. (1999) The structural basis for specificity of substrate and recruitment peptides for cyclin-dependent kinases, *Nat. Cell Biol. 1*, 438−443.
42. Sharrocks, A. D., Yang, S. H., and Galanis, A. (2000) Docking domains and substrate-specificity determination for MAP kinases, *Trends Biochem. Sci. 25*, 448−453.
43. Marangoni, A. G. (2003) *Enzyme Kinetics: A Modern Approach*, Wiley-Interscience, Hoboken, NJ.
44. Huynh, Q. K., Kishore, N., Mathialagan, S., Donnelly, A. M., and Tripp, C. S. (2002) Kinetic mechanisms of IkappaB-related kinases (IKK) inducible IKK and TBK-1 differ from IKK-1/IKK-2 heterodimer, *J. Biol. Chem. 277*, 12550−12558.
45. Burke, J. R., Miller, K. R., Wood, M. K., and Meyers, C. A. (1998) The multisubunit IkappaB kinase complex shows random sequential kinetics and is activated by the C-terminal domain of IkappaB alpha, *J. Biol. Chem. 273*, 12041−12046.
46. Peet, G. W., and Li, J. (1999) IkappaB kinases alpha and beta show a random sequential kinetic mechanism and are inhibited by staurosporine and quercetin, *J. Biol. Chem. 274*, 32655−32661.
47. Gold, M. H., and Segel, I. H. (1974) Neurospora crassa protein kinase. Purification, properties, and kinetic mechanism, *J. Biol. Chem. 249*, 2417−2423.
48. Cole, P. A., Burn, P., Takacs, B., and Walsh, C. T. (1994) Evaluation of the catalytic mechanism of recombinant human Csk (C-terminal Src kinase) using nucleotide analogs and viscosity effects, *J. Biol. Chem. 269*, 30880−30887.
49. Boerner, R. J., Barker, S. C., and Knight, W. B. (1995) Kinetic mechanisms of the forward and reverse pp60c-src tyrosine kinase reactions, *Biochemistry 34*, 16419−16423.

50. Cook, P. F., Neville, M. E., Jr., Vrana, K. E., Hartl, F. T., and Roskoski, R., Jr. (1982) Adenosine cyclic 3′,5′-monophosphate dependent protein kinase: kinetic mechanism for the bovine skeletal muscle catalytic subunit, *Biochemistry 21*, 5794−5799.
51. Horiuchi, K. Y., Scherle, P. A., Trzaskos, J. M., and Copeland, R. A. (1998) Competitive inhibition of MAP kinase activation by a peptide representing the alpha C helix of ERK, *Biochemistry 37*, 8879−8885.
52. Chen, G., Porter, M. D., Bristol, J. R., Fitzgibbon, M. J., and Pazhanisamy, S. (2000) Kinetic mechanism of the p38-alpha MAP kinase: phosphoryl transfer to synthetic peptides, *Biochemistry 39*, 2079−2087.
53. LoGrasso, P. V., Frantz, B., Rolando, A. M., O'Keefe, S. J., Hermes, J. D., and O'Neill, E. A. (1997) Kinetic mechanism for p38 MAP kinase, *Biochemistry 36*, 10422−10427.
54. Whitehouse, S., and Walsh, D. A. (1983) Mg X ATP2-dependent interaction of the inhibitor protein of the cAMP-dependent protein kinase with the catalytic subunit, *J. Biol. Chem. 258*, 3682−3692.
55. Erneux, C., Cohen, S., and Garbers, D. L. (1983) The kinetics of tyrosine phosphorylation by the purified epidermal growth factorreceptor kinase of A-431 cells, *J. Biol. Chem. 258*, 4137−4142.
56. Posner, I., Engel, M., and Levitzki, A. (1992) Kinetic model of the epidermal growth factor (EGF) receptor tyrosine kinase and a possible mechanism of its activation by EGF, *J. Biol. Chem. 267*, 20638−20647.

BI602423E